Computational Condensed Matter 28 (2021) e00582

Contents lists available at ScienceDirect

Computational Condensed Matter

journal homepage: www.elsevier.com/locate/cocom

Adsorption and coadsorption of H and Li on Ag(100) surface: DFT studies including dispersion correction

C.C. Boungou [a,*], G.B. Bouka-Pivoteau [a], B.R. Malonda-Boungou [a,b], M. N'dollo [a], P.S. Moussounda [a], A.T. Raji [c], E. Kanga [a]

[a] Groupe de Simulations numériques en Magnétisme et Catalyse (GSMC), Faculté des Sciences et Techniques, Université Marien NGOUABI, BP 69 Brazzaville, Congo

[b] Unité de Recherche en Nanomatériaux et Nanotechnologie, Institut National de Recherche en Sciences Exactes et Naturelles (IRSEN), Brazzaville, Congo

[c] Department of Physics, College of Science, Engineering and Technology (CSET), University of South Africa (UNISA-Florida Campus), Corner of Christiaan de Wet Road & Pionner Avenue, Florida 1709, South Africa

ARTICLE INFO

Keywords:
Density functional theory (DFT)
van der waals
Hydrogen
Lithium
Silver
Adsorption and coadsorption

ABSTRACT

We report on the results of DFT calculations of H, Li adsorption and Li+H coadsorption on Ag(100) surface. By using the GGA–PBE functional and DFT+$d3$, we obtain the adsorption energies, coadsorption energies, structural parameters, work function change and dipole moments. Our GGA–PBE calculations show that H prefers the bridge site at 0.25 and 0.50 ML coverages but hollow site at 0.75 and 1.00 ML coverages. With the DFT+d3 functional, we find that H is most stable at bridge site at 0.25 ML coverage, however, it prefers the hollow site at 0.50 ML, 0.75 ML and 1.00 ML coverages. For Li adsorption, both GGA–PBE and DFT+d3 functionals show that Li is most stable at hollow site. For Li and H coadsorption, we find that Li at the hollow site with H at the nearest-neighbor bridge site as the most energetically favorable configuration. The evolution of local electronic structures of the adsorbates and Ag(100) surface has been analyzed in terms of local density states. Our calculations show a decrease in the work function when Li and H are coadsorbed on the Ag(100) surface which suggests a possible transfer of electron from the Li-H adsorbates to the Ag(100) surface.

1. Introduction

In a fuel cell electrode, the metal surface is where chemical reactions such as the hydrogen adsorption, diffusion and combination with oxygen and other chemical species take place [1,2]. This metal surface is often called catalytic surface and thus, the understanding of adsorption process of hydrogen on this surface is very important from experimental and theoretical point of view. Platinum has been generally used as the catalytic surface in fuel cells, however, some previous studies have proposed alternative catalysts, in particular transition metals. Likewise, several theoretical studies of H adsorption on metal surfaces have been reported. As examples, adsorption of H has been studied on Ag (100) [3–8] and Ag(111) surfaces [6,9,10]. Eichler et al. [3], Jung and Kang [5], Ferrin et al. [6], Gòmez et al. [7] and Sanchez et al. [8], using the density functional theory (DFT) approach, have studied H adsorption on Ag(100) surface. These previous studies [3,5,7,8] found that the hollow site is the most stable site. This however contradicts the work of Ferrin et al. [6] who found that the bridge site is the preferred H adsorption site. Also, configuration interaction (CI) theoretical approach has been used by Qin and Whitten to investigate adsorption of H on Ag(100) surface [4]. They have reported that the hollow site is the preferred site. In addition, DFT studies of H on Ag(111) surface, show that the hollow-fcc site is the most energetically favorable site [6,9,10]. Furthermore, chemisorption of H on Au (100) surface has been studied by Ferrin et al. [6], Gòmez et al. [7] and N'dollo et al. [11]. When combined, the works of these authors show that the preferred adsorption site of H on Au(100) surface remain questionable. While the bridge site is obtained as the most stable site in Ref. [6,7], the top site (four layers) is obtained by N'dollo et al. [11].

Adsorption of H on Au(111) surface has been reported in the Refs. [6,12], where the hollow-fcc site has been shown to be the most stable site for the H adsorption. Also, the adsorption of H on Rhodium surface have been studied on the Rh (100) [3,6] and Rh (111) surfaces [6,13,14]. Refs. [3,6] have shown that H is most stable on hollow site while Refs. [6,13,14] suggest that the most likely H adsorption site is the hollow-fcc site. In addition, the interaction between H and Pd surface has been elucidated by several workers [3,5,6,15,16]. Eichler et al. [3] and Ferrin et al. [6] found that H is most stable on the hollow site of the Pd(100) surface. Besides, on the Pd(111) surface, H

* Corresponding author.
E-mail address: boungoucedric@yahoo.fr (C.C. Boungou).

https://doi.org/10.1016/j.cocom.2021.e00582
Received 21 April 2021; Received in revised form 12 July 2021; Accepted 30 July 2021
Available online 10 August 2021

preferential adsorbs on hollow-fcc site [6,15]. H adsorption has been also examined on Pt [6,7,14,16–20], Cu [6–8,21–24], Ni [6,16,25,26], Re [6,27], Ru [6,28], Fe [6,29–31] and Ir [6,32]. Gomes et al. [7], Mousounda et al. [17] and Saad et al. [18] using the DFT, have shown that H is most stable at bridge site of Pt(100) surface. Ferrin et al. [6], Xu et al. [29] and Jiang et al. [30] have shown that the preferred adsorption site of H on Fe(110) surface is the hollow site. Theoretical studies of adsorption of H on bimetallic surfaces have also been performed. Matczak et al. [33], using DFT and cluster model calculations, reported H adsorption on the (100) bimetallic surfaces like Pd-Ag, Pd-Pt, Pd-Au, Pt-Ag and Pt-Au. This study predicts H on the top site as the most likely adsorption location.

Experimental studies of H adsorption on the metal surfaces have also received significant attention. Experimental techniques such as the high-resolution electron energy loss spectroscopy (HREELS) [34], temperature-programmed desorption (TPD) [34] and low-energy electron diffraction (LEED) [35] have been employed to study H chemisorption on Ag(111) surface. The studies [34,35] show that H prefers hollow sites. The same experimental techniques were used in the adsorption studies of H on Ni [36–39], Fe [40–42], Pd [43–46], Pt [47,48], Ru [49], Cu [50–53], Rh [54] and Ir [55,56]. Studies of alkali atom adsorption on metal surfaces in particular, serves as a model which may enable us to understand more complicated systems. This has motivated studies of Li adsorption on Pt(100), Pt(110) and Pt(111) surfaces [18] using the DFT approach and the slab model. Platinum has always been of interest due to its extensive applications such as in catalysis and hydrogenation of olefins. In Ref. [18], it was concluded that, at coverage of 0.25 ML (mono-layer) in a p(2 × 2) unit cell, lithium preferentially adsorbs on hollow, hollow and hollow (fcc) sites on Pt(100), Pt(110) and Pt(111) surfaces, respectively. Also, Ohsaki and Oguchi [57] have performed first-principles calculations to study the stability of Li adsorbed on Cu(001) surface and found that in the Cu(001)-Li system, the (2 × 1)s structure is more stable than the c(2 × 2)s structure. In addition, Mannstadt [58] reported the DFT calculations of the work function change upon adsorption of Li on Ru(100) surface. Experimentally, adsorption of Li, Na and K alkali atoms on metal surface have attracted significant attention. For example, adsorption of Li on Ag(100) [59], Ag(110) [60], Ag(111) [61], Cu(100) [57] and Al(110) [62] surfaces have been characterized using the experimental techniques such as, LEED [59,60,62], Auger electron spectroscopy AES [60,61], scanning tunneling microscopy (STM) [57] and core-level photoemission spectroscopy (CLS) [62], respectively. In particular, Ref. [61] focuses on the work function changes due to Li adsorption on the Ag(111) surface.

In this work, using the DFT approach (with and without dispersion correction) and the slab model, we study the adsorption of H and Li on the Ag(100) surface. Specifically, we determine the adsorption properties of each of H and Li on Ag(100) surface on the one hand, and the coadsorption of Li and H on the Ag (100) surface on the other hand. The Li and H adsorption and their coadsorption are studied at various sites and coverages. Our choice of Ag is borne out of the fact that it is a catalyst which is used in numerous industrial processes such as the partial oxidation of methanol to formaldehyde, ammonia oxidation and ammonia synthesis from nitrogen and hydrogen. We also remark that experimental data on hydrogen atom adsorption on Ag(100) surface is not yet available. Therefore, in view of potential use of Ag as an alternative to Pt in various applications involving H production such as in fuel cells and industrial catalytic processes, it is pertinent to perform theoretical studies to elucidate the adsorption properties of H as well as H coadsorption with Li on the Ag(100) surface. The latter enables us to determine the influence of Li on the H adsorption and vice-versa. An earlier study similar to ours is the work of Saad et al. [18] who, using DFT approach and the slab model, investigated the coadsorption of H and Li on (100), (110) and (111) surfaces of platinum. Our paper is structured as follows: In Section 2, we present the details of theoretical methods used in this work. Section 3 reports the results on basic structural and electronic properties of relaxed clean Ag(100) (Section 3.1), adsorption of H on Ag(100) surface (Section 3.2); adsorption of Li on Ag(100) surface (Section 3.3) and coadsorption of H and Li on Ag(100) (Section 3.4). In the last section (Section 4), we present the major conclusion of this work.

2. Computational method

All calculations presented in this work have been performed using the Quantum Espresso software package [63]. We have employed the generalized gradient approximation (GGA) of the Perdew–Burke–Ernzerhof (GGA–PBE) [64] flavor as the exchange–correlation functional. We also studied the effect of dispersion-correction on the calculated properties by using the non-local van der Waals functional, i.e., DFT+d3, as proposed by Grimme et al. [65]. We shall hereafter refer to GGA–PBE functional with the vdW+d3 dispersion correction as PBE+d3. The ionic cores were described by ultrasoft pseudopotentials with scalar relativistic corrections as constructed by the Rappe–Rabe–Kaxiras–Joannopoulos (RRKJUS) method. Plane waves basis with kinetic energy cutoff of 400 eV have been used to solve the Kohn–Sham equations for the valence electrons. Brillouin zone integration is performed using the Monkhorst–Pack [66] grid of size 12 × 12 × 1 and 6 × 6 × 1 for the (1 × 1) and (2 × 2) supercells respectively used in the calculations. The Ag(100) surface has been modeled using the slab geometry. We used four layers of Ag slab and the adsorbates have been placed on the topmost layer of slab. We found a good convergence of our calculations with a vacuum of 12 Å between two consecutive slabs. Also, in this study, four coverages (θ) have been investigated. The 0.25, 0.5 and 0.75 monolayer (ML) coverages for (2 × 2) unit cell and 1.00 ML for (1 × 1) unit cell. Also, three adsorption sites have been considered the top, bridge and hollow sites, as shown in Fig. 1. The adsorbate and the top layer of slab have been completely relaxed in our study. The total energy of isolated adsorbate, i.e, Ag or H or Li atoms was obtained using a cubic box of dimensions 10 Å × 10 Å × 10 Å and a k-points grid of 1 × 1 × 1 (Γ-point). Increasing the size of the cubic cell beyond this cell size does not change the total energies by more than 20 meV. The force convergence criteria is a threshold of less than 10^{-5} eV/Å. The geometric optimization has been performed using the BFGS quasi-Newton algorithm.

The bulk modulus (B_0) is an important mechanical parameter which may give an indication of the accuracy of the exchange–correlation functionals that we have used. The B_0 is extracted from the Birch–Murnaghan [67] equation of state (EOS). Also, the cohesive energy which gives an indication of the stability of the bulk system against the constituents chemical elements is calculated from the expression:

$$E_{coh} = E_{\mathrm{Ag}} - E_{bulk}/N \tag{1}$$

where E_{Ag} denotes the energy of an silver isolated atom; E_{bulk} is the energy of the bulk and N denotes the number of atoms contained in the bulk.

The surface energy has been determined using the following equation:

$$E_{surf} = \frac{1}{2A}(E^{N'}_{slab} - N' E'_{bulk}) \tag{2}$$

where $E^{N'}_{slab}$ is the total energy of the clean slab containing N' atoms, A the area of the surface unit cell and E'_{bulk} is the energy per atom in the bulk.

The change in interlayer spacing (in percentage) is defined according to formula:

$$\Delta d_{ij} = 100\frac{d_{ij} - d_0}{d_0} \tag{3}$$

where d_{ij} is the distance separating the relaxed interlayer i and j, and d_0 is the unrelaxed interlayer distance ($d_0 = \frac{a_0}{2}$).

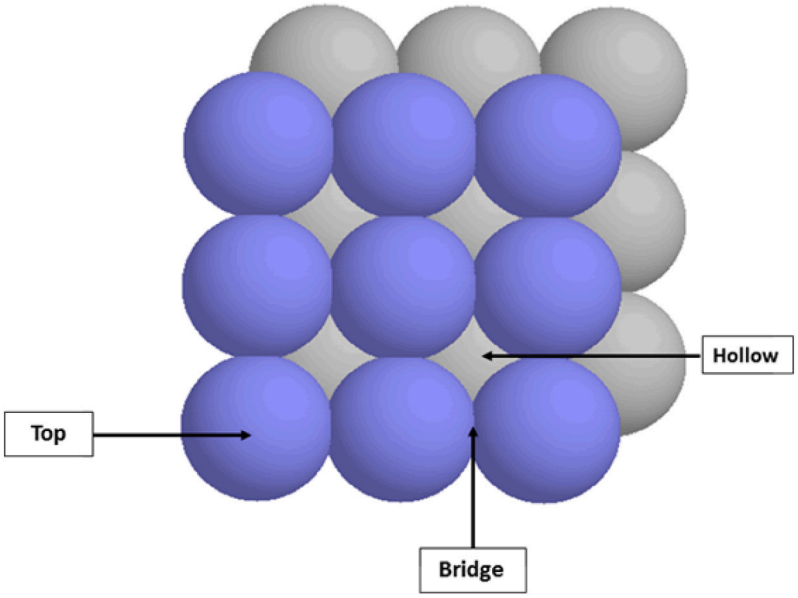

Fig. 1. Top view of a Ag(001) surface in the (2 × 2) unit cell with three high-symmetry adsorption sites labeled: top, bridge and hollow sites. In blue and dark colors are the Ag atoms on the first and second layers, respectively. (For interpretation of the references to color in this figure legend, the reader is referred to the web version of this article.)

The adsorption energy (E_{ads}) was computed using the equation:

$$E_{ads} = \left(E_{adsorbate/\mathrm{Ag}(100)} - E_{\mathrm{Ag}(100)} - n \times E_{adsorbate}\right)/n \quad (4)$$

where $E_{adsorbate/\mathrm{Ag}(100)}$ is the total energy of the adsorbate–Ag (100) system, $E_{\mathrm{Ag}(100)}$ represents the total energy of the clean Ag(100) slab and $E_{adsorbate}(adsorbate = \mathrm{H, Li})$ denotes the total energy of the isolated adsorbate and n corresponds to number of adsorbates located on the surface. In this convention, a negative E_{ads} value corresponds to a favorable adsorption.

The work function change ($\Delta\Phi$) is defined as follows:

$$\Delta\Phi = \Phi_{adsorbate/\mathrm{Ag}(100)} - \Phi_{\mathrm{Ag}(100)} \quad (5)$$

where $\Phi_{adsorbate/\mathrm{Ag}(100)}$ is the work function of the adsorbate–Ag(100) system and $\Phi_{\mathrm{Ag}(100)}$ the work function of clean Ag(100) slab. The work function may be explained as the minimum energy needed by an electron to escape from a solid through a particular surface and it is crystallographic orientation dependent. Work function changes are an important source of information in the study of adsorbates interaction with a solid surface.

The surface dipole moment (in Debye) is evaluated by using the Helmholtz formula:

$$\Delta\mu = \frac{A\Delta\Phi}{12\pi\theta} \quad (6)$$

where A is the area per (1 × 1) surface unit cell in Å^2, $\Delta\Phi$ is the work function change in eV and θ is the coverage.

The coadsorption energy of H and Li has been obtained using the following equation:

$$E_{coads} = E_{(\mathrm{H+Li})/\mathrm{Ag}(100)} - E_{\mathrm{Ag}(100)} - E_{\mathrm{H}} - E_{\mathrm{Li}} \quad (7)$$

where $E_{(\mathrm{H+Li})/\mathrm{Ag}(100)}$ represents the total energy of H+Li on Ag(100) surface and E_{H} and E_{Li} are the total energies of the H and Li in the isolated phase. According to this definition, a negative E_{coads} value means favorable coadsorption.

The coadsorption energy of H adsorbed on the Ag(100) surface in presence of Li is calculated using the equation:

$$E^{\mathrm{H}}_{coads} = E_{(\mathrm{H+Li})/\mathrm{Ag}(100)} - E_{\mathrm{H}} - E_{\mathrm{Li}/\mathrm{Ag}(100)} \quad (8)$$

where $E_{\mathrm{Li/Ag}}$ corresponds to the total energy of Li on Ag(100) surface.

The coadsorption energy of Li adsorbed on the Ag(100) surface in presence of H was calculated using equation:

$$E^{\mathrm{Li}}_{coads} = E_{(\mathrm{H+Li})/\mathrm{Ag}(100)} - E_{\mathrm{Li}} - E_{\mathrm{H}/\mathrm{Ag}(100)} \quad (9)$$

where $E_{\mathrm{H/Ag}}$ corresponds to the total energy of H on Ag(100) surface.

3. Results and discussion

Before discussing results on the adsorption of H, Li and H+Li coadsorption on Ag(100) surface, we firstly present the results on properties of bulk and clean surface of Ag(100) and compare with previous experiment and theoretical studies, where available. This will enable us to determine how well our calculation parameters are able to reproduce the well-known results and to determine the relatively unknown properties of H/Ag(100), Li/Ag(100) and (H+Li)/Ag systems.

3.1. Bulk and clean Ag surface properties

Table 1 shows the calculated mechanical properties (lattice constant (a_0), bulk modulus (B_0) and cohesive energy (E_{coh})) obtained in the present work, and compared with other theoretical values as well as available experimental data.

Our calculated a_0 for the bulk fcc Ag as obtained with the GGA–PBE and PBE+d3 only differs by 0.07 Å; i.e., 4.18 Å and 4.11 Å respectively. These values compare reasonably with the experimental values of 4.09 Å [75] and 4.07 Å [76] with the PBE+d3 slightly in better agreement with the experiment. Also, our PBE value of a_0 is in good agreement with previous reported PBE and PW91 values which vary between 4.14 Å and 4.17 Å, as reported in the Refs. [3,7,9,68–73]. Furthermore, having established that the a_0 values obtained with the GGA and PBE+d3 may differ, albeit slightly, we should also emphasize that different variants of vdW dispersion corrections may give values of a_0 which differ from the experiment by different amount, as shown for the vdW-DF, vdW-DF2, vdW-DF-cx, optPBE-vdW and C09x-vdW in Table 1. Also, we have obtained the bulk modulus value of 102.84 GPa with the PBE functional. This is in good agreement with the experimental data [75,76], as shown in Table 1. However, PBE+d3 calculations gives a bulk modulus value of 94.7 GPa. These values are to be compared with the 100.7 GPa and 105.7 GPa as reported in the experiment (cf. Table 1). Similar to the case of a_0, we note

Table 1
Bulk properties obtained in the present work, compared with other theoretical and experimental data. The table summarizes theoretical data obtained using the GGA (GGA-PW91 and GGA–PBE) as well as different types of van der Waals (vdW) dispersion corrections.

	a_0 (Å)	B_0 (GPa)	E_{coh} (eV)
Present work (GGA–PBE)	4.18	102.8	2.57
Present work (PBE+d3)	4.11	94.7	2.99
PW91 [3]	4.17	–	–
PBE [7]	4.16	89.6	2.61
PW91 [9]	4.14	–	–
PW91 [68]	4.14	96.0	–
PBE [69]	4.16	91.2	2.51
PBE [70]	4.15	91.1	2.53
PBE [71]	4.16	91.0	2.55
PBE [72]	4.16	101.0	–
PBE [73]	4.16	–	–
PBE [74]	–	83.3	2.49
PBE+vdW-D [69]	4.26	79.9	2.15
PBE+vdW-DF2 [69]	4.28	108.8	2.02
PBE+vdW-DF-cx [69]	4.10	110.5	2.95
PBE+vdW-DF2 [70]	4.36	58.6	2.15
PBE+optPBE-vdW [70]	4.23	78.2	2.52
PBE+C09x-vdW [70]	4.10	110.9	3.06
Experimental value [75]	4.09	100.7	2.95
Experimental value [76]	4.07	105.7	2.96

Table 2
Properties (work function (Φ), surface energy (E_{surf}), and change in interlayer distance (Δd_{ij})) of clean Ag surface obtained in the present work, compared with other theoretical and experimental data. The values in parenthesis correspond to those obtained for the (1 × 1) unit cell while values that are not in parenthesis are data obtained for (2 × 2) unit cell.

	Φ (eV)	E_{surf} (J/m^2)	Δd_{12} (%)	Δd_{23} (%)
Present work (PBE)	4.21 (4.21)	0.82 (0.82)	−1.84 (−1.88)	−0.58 (−0.62)
Present work (DFT-d3)	4.24 (4.24)	1.24 (1.24)	0.27 (−0.20)	1.39 (0.15)
PW91 [3]	4.31	–	−2.00	–
PW91[68]	4.21	–	–	–
PBE [70]	–	0.74	–	–
PBE [71]	4.14	0.840	−2.26	−0.100
PBE [72]	4.18	0.80	−2.0	+ 0.82
PBE [78]	(4.25)	(1.267)	–	–
PW91 [79]	4.22	–	−1.90	+ 0.60
PBE [80]	4.23	–	−1.60	+ 0.90
PW91 [87]	–	0.842	–	–
PBE+vdW-DF2 [70]	–	0.55	–	–
PBE+optPBE-vdW [70]	–	0.80	–	–
PBE+C09x-vdW [70]	–	1.12	–	–
PBE+vdW-DF [73]	4.11	–	–	–
Experimental value [77]	4.22 ± 0.44	–	–	–
Experimental value [78]	4.64	1.25[a]	–	–
Experimental value [82]	–	–	0.0 ± 1.5	0.0 ± 1.5

[a]Value measured on Ag(111) surface.

that different variants of vdW dispersion corrections give B_0 that are at varying degree of accuracy compared to the experiment. It is suffice to say that in this work, the PBE gives a value of B_0 that is more in agreement with the experiment compared to the PBE+d3. It is important to also emphasized that in general, a more extensive calculations, beyond the focus of this work, is needed to determine the influence of vdW corrections on the mechanical properties of Ag. In the following, we shall adopt a_0 value of 4.18 Å for the PBE calculations and 4.11 Å for the PBE+d3 calculations. Furthermore, we calculated the cohesive energy (E_{coh}) as 2.57 eV and 2.99 eV which are obtained using the GGA–PBE and PBE+d3 functionals respectively. Our PBE value is in excellent agreement with similar PBE calculations in Refs. [7,69–71,74], as shown in Table 1. Also, our PBE+d3 calculated E_{coh} is in excellent agreement with the experimental value of 2.95 eV [75] and 2.96 eV [76], and with DFT+vdW-DF-cx calculations performed by Ambrosetti and Silvestrelli [69]. Finally, we have obtained a positive value for the E_{coh} which confirms the stability of the bulk of Ag and the appropriateness of our calculations parameters.

A quantitative study of surface properties consists in determining parameters such as the work function (Φ), surface energy (E_{surf}), and change in interlayer distance (Δd_{ij}) after relaxation. Our calculated values for the clean Ag surface properties as obtained in the present work and the comparison with other theoretical and experimental data are shown in Table 2. The Table 2 shows that the inclusion of vdW interactions considerably modifies surface energy and change in interlayer distance compared to ordinary PBE. This Table 2 shows that the work function value obtained from PBE calculations and PBE+d3 are generally in good agreement with the experiment [77], and are consistent with other previous DFT studies [3,68,71,72,78–80]. With regard to the surface energy, experimental values of 0.80 J/m^2 [81] and 1.250 J/m^2 [82] have been reported. Our PBE value of 0.82 J/m^2 is in excellent agreement with Ref. [81] while the PBE+d3 value of 1.24 J/m^2 is also in excellent agreement with Ref. [82]. Previous PBE values are within the range of 0.74 J/m^2 to 1.27 J/m^2. The inclusion of different types of vdW corrections as reported in previous studies show the value of surface energy in the range 0.55 J/m^2–1.12 J/m^2. It suffices to say the value of surface energy that we have obtained in this study, either with PBE or PBE+d3 are consistent with the values reported in the experiment. Also, we observed that in the case of PBE calculated values of interlayer distance, the unit cell size has no effect on the change in the interlayer distance after relaxation. An opposite trend is observed for the PBE+d3 calculations. In addition, for the PBE calculations, the changes in the topmost interlayer spacing (Δd_{12}) are −1.84% (−1.88%) and −0.58% (−0.62%), for the 2 × 2 (1 × 1) unit cells, respectively. These values are in good agreement with previous PBE calculations [3,71,72,79,80]. However, experiment [82] finds no relaxation in the first interlayer spacing, i.e., Δd_{12} equals 0.0 ± 1.5%. Nevertheless, at this point we find it useful to compare our calculated values for the change in the relaxed first (Δd_{12}) and second interlayer spacings (Δd_{23}) with similar fcc(100) metal surfaces such as Cu and Pd, as reported in other studies. For example, Refs. [83,84] found the values of -1.1 ± 0.4% and 3.1 ± 1.5% for Δd_{12} in Cu(100) and Pd(100) surfaces, respectively. Similar results have been reported by Oed et al. [85,86] for the first interlayer spacing in Ni(100), i.e., $\Delta d_{12} = -1 \pm 1$%) and Rh (100) where $\Delta d_{12} = -0.9 \pm 2$%. Therefore, within the experimental error, our calculated interlayer spacing Δd_{12} for the Ag(100) surface are within the range usually obtained for fcc (100) transition-metal surfaces.

3.2. Adsorption of H on Ag(100) surface

3.2.1. Adsorption energies and structural parameters

Here, we present the results on the adsorption energies (E_{ads}), structural parameters (i.e., distance between the H and Ag, $d_{\mathrm{H-Ag}}$), work function change ($\Delta\Phi$) and dipole moment due to H adsorption on Ag(100) surface ($\Delta\mu$). As stated earlier, the three adsorption sites for H have been considered top, bridge and hollow, and these have been studied as a function of H coverage. These parameters are presented in Table 3.

All the adsorption energies (E_{ads}) are negative irrespective of the functional (GGA–PBE or PBE+d3) or the coverage (θ). This suggests that the adsorption of H on Ag(100) surface is favorable for all coverages and sites considered. The variation of (E_{ads}) as a function of θ curve for the *top*, *bridge* and *hollow* sites, are shown in Fig. 2. For each of the sites, the E_{ads} versus θ curve is qualitatively similar for the GGA–PBE and PBE+d3 functionals. Notably however, is the fact that the E_{ads} for the bridge and the hollow site is similar for all the coverages, and both are lower (i.e., more negative) than the E_{ads} for the top site. This clearly suggests that the H atom has higher possibility of being adsorbed on the bridge or hollow sites compared to the top site, for all the coverages. Nevertheless, certain points worth mentioning. Specifically, for the top site, the adsorption energy decreases (i.e., less

Table 3
Adsorption energies (E_{ads}), structural parameters (d_{H-Ag}), work function change ($\Delta\Phi$) and dipole moment ($\Delta\mu$) for H/Ag(100) system. The values obtained with GGA–PBE calculations are outside the parenthesis while those in the parenthesis are obtained with PBE+d3.

Evaluated parameters	Adsorption sites	H coverage (ML) 0.25	0.50	0.75	1.00
E_{ads} (eV)	Top	−2.49 (−2.55)	−2.33 (−2.40)	−2.29 (−2.35)	−2.238 (−2.302)
	Bridge	−2.92 (−2.98)	−2.93 (−2.98)	−2.90 (−2.94)	−2.86 (−2.908)
	Hollow	−2.89 (−2.96)	−2.91 (−2.99)	−2.91 (−2.99)	−2.88 (−2.953)
d_{H-Ag} (Å)	Top	1.67 (1.70)	1.66 (1.69)	1.66 (1.68)	1.65 (1.68)
	Bridge	1.82 (1.85)	1.80 (1.83)	1.79 (1.82)	1.79 (1.82)
	Hollow	2.12 (2.14)	2.12 (2.14)	2.12 (2.14)	2.11 (2.12)
$\Delta\Phi$ (eV)	Top	0.89 (0.83)	1.20 (1.13)	1.40 (1.32)	1.57 (1.49)
	Bridge	0.32 (0.31)	0.72 (0.69)	0.95 (0.93)	1.16 (1.13)
	Hollow	0.21 (0.03)	0.09 (0.08)	0.15 (0.01)	0.06 (0.03)
$\Delta\mu$ (Debye)	Top	0.83 (0.75)	0.56 (0.51)	0.43 (0.39)	0.36 (0.33)
	Bridge	0.30 (0.28)	0.33 (0.31)	0.29 (0.28)	0.27 (0.25)
	Hollow	0.20 (0.03)	0.05 (0.01)	0.05 (0.00)	0.01 (0.01)

negative) steeply when the coverage increases from 0.25 ML to 0.50 ML. However at coverages above 0.50 ML, the adsorption energy continues to decrease, but gradually. This trend may be adduced to repulsive interactions between the adsorbed atomic hydrogen atoms. Such a repulsion results in the H atom at the top site being less stable with increasing H coverage. The situation is different with the bridge and hollow sites. In this case, the E_{ads} versus θ curve is almost linear and there is no significant difference between the adsorption energies at both sites, i.e., only between 5 meV to 45 meV, as the coverage increases. Such a small energy difference (i.e., $\leq$ 0.05 eV) between the E_{ads} for the two sites (bridge and hollow), irrespective of the coverage, suggests that there is an equal possibility of H to be found at these two sites. Indeed, the bridge site preference of the adsorbed H atom at low coverage, of 0.25 ML and 0.50 ML, is consistent with the result of Ferrin et al. [6] on the same system. Also, we find similar observation in related work on H adsorption on Au(100) [6,7], Pt(100) [6,7,17,18] and Ir(100) [6] surfaces. It must be stated however that other studies as reported in Refs. [3–5,7,8] suggested a different preferred adsorption site of H on Ag(100).

Also of relevance is the work of Eichler et al. [3] who have used the DFT+PW91 and slab model to study the adsorption of H on Ag(100) surface and obtained adsorption energies of 1.27, 1.91 and 1.96 eV at top, bridge and hollow sites, respectively. The adsorption energies of 1.53, 1.62 and 1.85 eV at top, bridge and hollow sites, respectively, have been determined by Qin and Whitten, in configuration interaction (CI) approach of H adsorption on Ag(100) [4]. Our adsorption energies values at 0.25 ML coverage are on average, about 1 eV greater than those found by Eichler et al. [3] and Qin and Whitten [4]. Also, on H/Ag(100) system, Gomez et al. [7] reported the values −2.44 eV, −2.95 eV and −3.00 eV at top, bridge and hollow sites, respectively. Sanchez et al. [8] applied DFT calculations, Monte Carlo (MC) simulations and a Cluster-exact Approximation(CA) to study H/Ag(100) system and reported the adsorption energies of −2.78, −3.36 and −3.29 eV at top, bridge, hollow sites, respectively. The values reported by Gomez et al. and Sanchez et al. [7,8] are in good agreement with ours results. These studies [7,8] suggest that the bridge or the hollow sites could be the preferred H adsorption site in H/Ag(100) system, consistent with our PBE and PBE+d3 calculations. Furthermore, the structural parameter, d_{H-Ag} varies between 1.65 and 2.12 Å (PBE) and 1.68 and 2.14 Å (PBE+d3 calculations). We find that for a given coverage, the separation d_{H-Ag} increases with the coordination number such that the separation is the biggest at the hollow site and lowest at the top site. Similar trend has been reported for H adsorption on Ag(100) [3,4], Pt(100) [18], Pt(110) [18], Pt(111) [18] and Fe(110) [30] surfaces. The distance d_{H-Ag} of 1.66, 1.79 and 2.11 Å at top, bridge and hollow sites have been calculated by Eichler et al. [3]. Qin and Whitten who have studied adsorption of H on Ag(100), found values 1.95, 2.08 and 2.18 Å for equilibrium distances d_{H-Ag}. The values reported by the Refs. [3,4] are in good agreement with our calculated values.

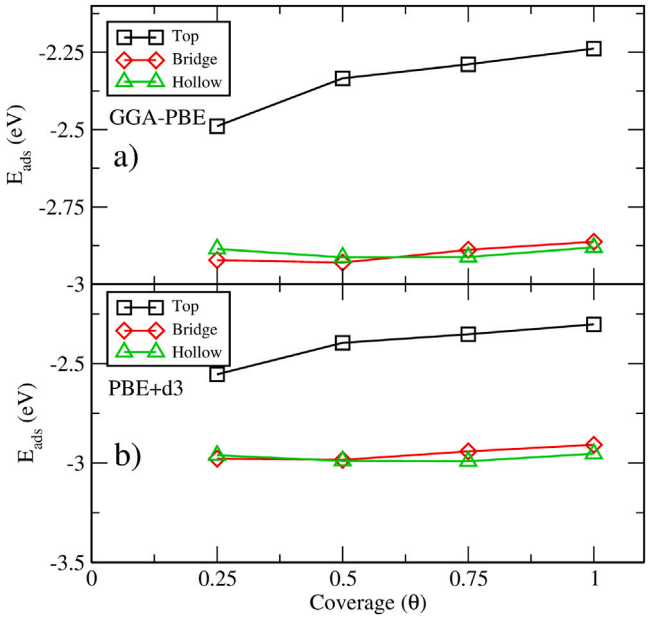

Fig. 2. Adsorption energy as a function of H coverage (ML) at Top, Bridge and Hollow sites. (a) PBE+GGA and (b) PBE+d3 (For interpretation of the references to color in this figure legend, the reader is referred to the Web version of this article).

3.2.2. Work function change and dipole moment of Ag(100) surface

The work function change is an important parameter in the calculations of surface properties [88]. It has been reported in the Ref. [30] that, when an atom which is more electronegative than the surface atoms is adsorbed on a surface, the adsorbed atom increase the work function of adsorbate–surface system. Consequently, following Eq. (5), the work function change is a positive value. On the contrary, an adsorbate which has a lower electronegativity than surface atoms decreases the work function of adsorbate–surface system, thus resulting in negative work function change. The electronegativity values of H, Li and Ag are 2.2, 0.98 and 1.93, respectively. Thus, as remarked in the Ref. [30], we expect an increase in work function of Ag (100) surface as a result of adsorption of H. Aside, one may speculate that the structural influence of hydrogen when adsorbed on the Ag(100) surface is accompanied by electronic charge redistribution within the surface which might lead to the change of the electronic work function, as we have observed. The values of work function change reported in Table 3 show in particular that the work function change increases when the coverage increases for top and bridge sites. This suggests that since the top and the bridge sites have different coordination (number of

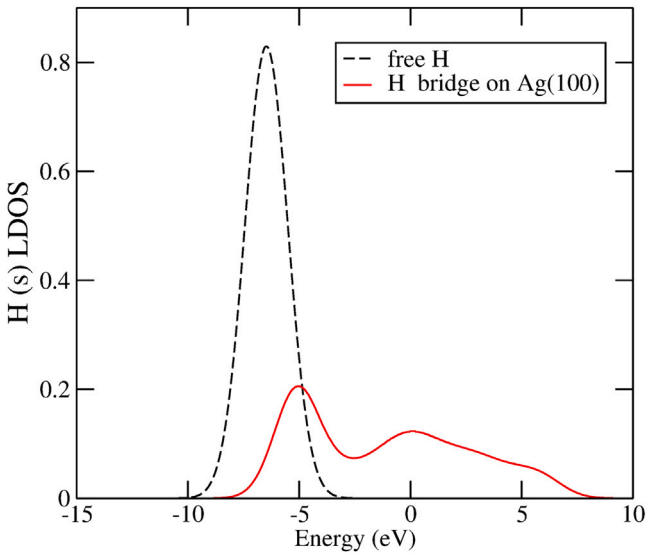

Fig. 3. (Color online) LDOS of s orbital of adsorbed H at the bridge site on Ag(100) surface and LDOS of H free. The zero energy denotes the Fermi level.

nearest-neighbor atom to the adsorbate), there is a correlation between work function change and the coordination number for all coverages considered. Indeed, a similar behavior has been observed in the studies of NCO adsorption on Cu(100) [89], Pd(100) [90] and Ag(100) [68]. Also, the $\Delta\Phi$ most significant value appears at 1.00 ML coverage for the top site. Concerning the dipole moment $\Delta\mu$, we notice that, for a given site the coverage dependence is not the same. However, $\Delta\mu$ decreases with increasing θ coverage for the top (PBE and PBE+d3 calculations) and hollow sites (PBE calculations). The dipole moment follows the following trend: $\Delta\mu_{hollow} < \Delta\mu_{bridge} < \Delta\mu_{top}$. The dipole moment enables us to determine the adsorbate–substrate dipole orientation. A positive value of dipole moment indicate that the H-Ag dipole is orientated toward surface.

3.2.3. Local Density of States (LDOS)

Here, we describe the electronic states induced by the H adsorption on Ag atoms, via the LDOS. Fig. 3 shows s orbital resolved LDOS of H and Ag atoms for the most stable site (i.e., bridge). We limit the LDOS calculations to the case of PBE and 0.25 ML coverage to demonstrate the nature of electronic interactions. From Fig. 3, one can observe a displacement toward the higher energies of s orbital after adsorption when compared with the LDOS of free hydrogen atom. Also, there is a decrease in the intensity of the peak situated at −6.56 eV in the free H LDOS after its adsorption on Ag(100). Indeed, this peak has an intensity of 0.82 e^- in free hydrogen and 0.20 e^- (situated at −5.24 eV) in adsorbed H on Ag(100) surface. Upon H adsorption, the LDOS of H shows the appearance of a new peak at −0.20 eV. The latter is absent in the free hydrogen LDOS. The shifting and reduction of the H peak, as well as the appearance of additional peaks indicate the hybridization between the s orbital of H and the Ag bands.

Fig. 4 shows the comparison of the projected density of states (PDOS) of the bare surface Ag prior H adsorption and the PDOS after H adsorption. From Fig. 4, the s, p_y and d_{xx-yy} bands of Ag move toward the lower energies, showing the stability of the system. If Figs. 3 and 4 are compared, one will notice that there is a strong hybridization between the s orbital H and s, p and d bands of Ag between −10 eV and 5 eV, which suggest that the H atom is indeed stable at the bridge site.

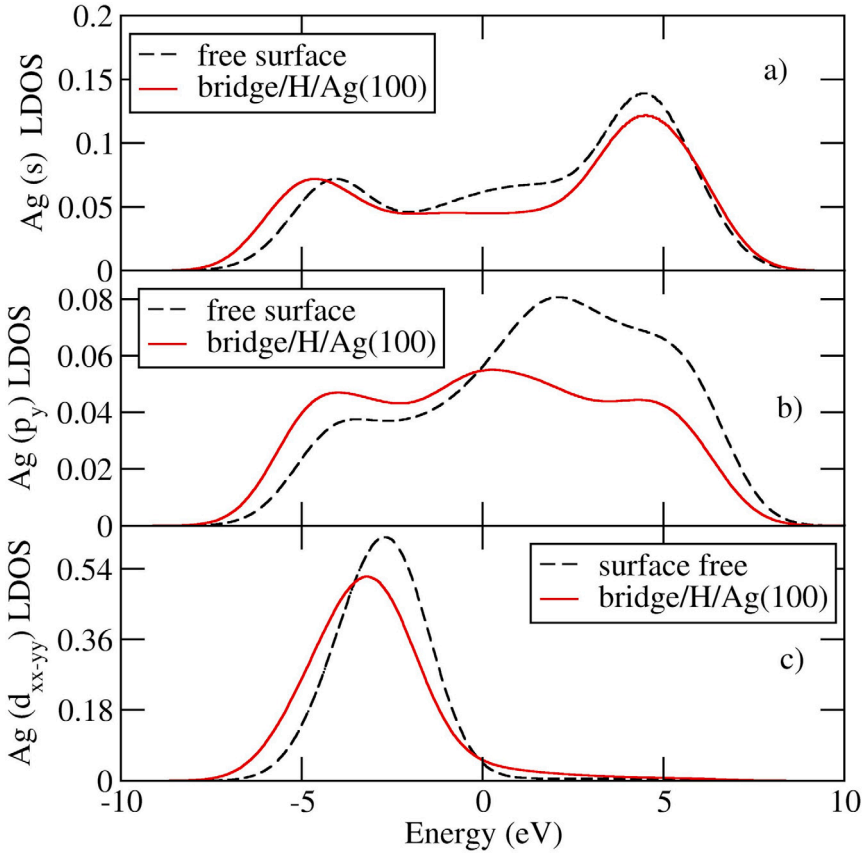

Fig. 4. (Color online) LDOS s and PDOS p_y and d_{xx-yy} of Ag band after H adsorption on Ag(100) surface and LDOS s and PDOS p_y and d_{xx-yy} of Ag band of the bare surface. The zero energy denotes the Fermi level.

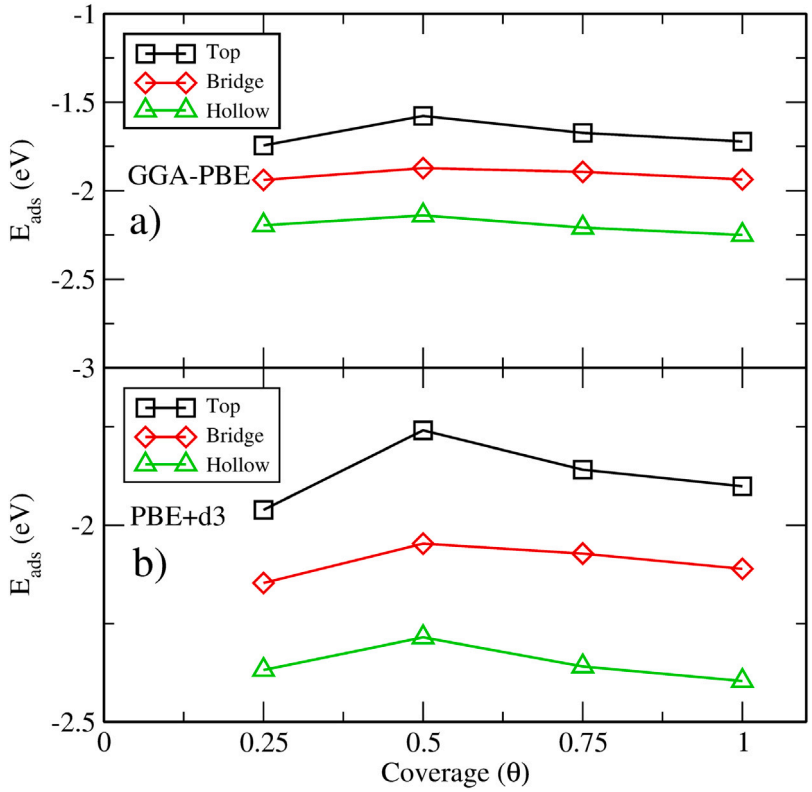

Fig. 5. Adsorption energy as a function of Li coverage (ML) at Top, Bridge and Hollow sites. (a) PBE+GGA and (b) PBE+d3 (For interpretation of the references to color in this figure legend, the reader is referred to the Web version of this article).

Table 4
Adsorption energies (E_{ads}), structural parameters (d_{Li-Ag}), work function change ($\Delta\Phi$) and dipole moment ($\Delta\mu$) for Li/Ag(100) system. The values obtained with DFT–PBE calculations are outside parenthesis and in the parenthesis are listed the results with PBE+d3.

Evaluated parameters	Adsorption sites	Li coverage (ML) 0.25	0.50	0.75	1.00
E_{ads} (eV)	Top	−1.74 (−1.96)	−1.58 (−1.76)	−1.67 (−1.86)	− 1.72 (−1.90)
	Bridge	−1.94 (−2.15)	−1.87 (−2.05)	−1.89 (−2.07)	−1.94 (−2.111)
	Hollow	−2.20 (−2.37)	−2.14 (−2.29)	−2.21 (−2.36)	−2.25 (−2.40)
d_{Li-Ag} (Å)	Top	2.46 (2.46)	2.48 (2.50)	2.55 (2.58)	2.59 (2.61)
	Bridge	2.60 (2.63)	2.60 (2.62)	2.58 (2.61)	2.68 (2.69)
	Hollow	2.77 (2.79)	2.73 (2.75)	2.77 (2.81)	2.75 (2.78)
$\Delta\Phi$ (eV)	Top	−0.48 (−0.50)	−0.33 (−0.36)	−0.22 (−0.23)	−0.11 (−0.12)
	Bridge	− 0.41 (−0.50)	−0.36 (−0.39)	−0.28 (−0.29)	−0.19 (−0.20)
	Hollow	− 0.31 (−0.33)	−0.31 (−0.34)	−0.31 (−0.34)	−0.30 (−0.31)
$\Delta\mu$ (Debye)	Top	−0.44(−0.31)	−0.15 (−0.30)	−0.07 (−0.07)	−0.03 (−0.03)
	Bridge	−0.38 (−0.31)	−0.17 (−0.30)	−0.09 (−0.07)	−0.04 (−0.05)
	Hollow	−0.29(−0.30)	−0.29 (−0.30)	−0.07 (−0.07)	−0.07 (−0.07)

3.3. Adsorption of Li on Ag(100) surface

3.3.1. Adsorption energies and structural parameters

The adsorption energies (E_{ads}), structural parameters (d_{Li-Ag}), work function change ($\Delta\Phi$) and dipole moment change ($\Delta\mu$) for Li/Ag(100) system are shown in Table 4. The adsorption energies have been obtained using the GGA–PBE and PBE+d3 functionals. Also shown in Fig. 5 are the variation of Li adsorption energies for the three adsorption sites (i.e., top, bridge, and hollow) as a function of the coverage (θ). The E_{ads} are all negative for all the coverages which suggests that Li is stable at either of the three sites (cf. Table 4 and Fig. 5). However, Li at the hollow site of Ag (100) has the strongest adsorption, i.e., most negative E_{ads} and thus, it is the most stable configuration. This conclusion is irrespective of the functional used. The preference of the hollow site may be explained by the fact that coordination number (CN) of Li at the hollow site is higher than at the bridge and top sites. Thus, Li is able to form multiple bonds with the higher number of coordinating atoms and thus has higher stability. Li at the top site has the least CN and thus the least E_{ads}. Also, it is observed that for each site, the adsorption energies decreases (i.e., less negative) when the coverage increases from 0.25 ML to 0.50 ML, then increases (i.e., more negative) slightly between 0.50 ML and 0.75 ML, before finally having an almost constant value between 0.75 and 1.00 ML. In addition, we observe that for all the coverages, the adsorption is stronger (i.e., more negative E_{ads}) with the PBE+d3 than the PBE functional, as shown in Table 4. Furthermore, to the best of our knowledge, no theoretical and experimental data have been reported on the adsorption energy of Li on the Ag(100) surface. However, Saad et al. [18] and Sorescu [91] have performed the DFT calculations to compute the adsorption energy of Li and K on the Pt(100) and Fe(100)

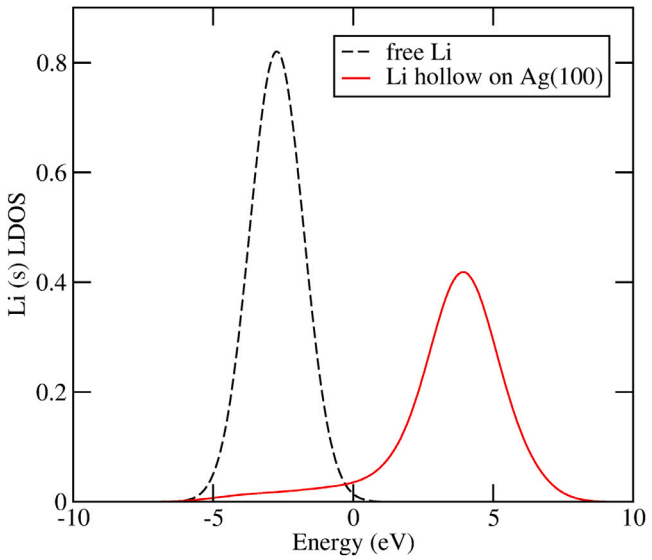

Fig. 6. (Color online) LDOS of s band of adsorbed Li at the bridge site on Ag(100) surface and LDOS of Li free. The zero energy denotes the Fermi level.

surface, respectively. In the case of Li/Pt(100) system, using DFT+GGA-PW91 and the slab model, Saad et al. [18] have obtained the adsorption energy values of −0.67 eV, −0.85 eV and −1.00 eV for the top, bridge and hollow sites, respectively, at 0.25 ML coverage. On the other hand, Sorescu [91] has investigated the adsorption of K on the bare Fe(100) surfaces, using GGA–PBE functional with periodic slab model. This author [91] reported the adsorption energies of −1.37 eV, −1.41 eV and −1.46 eV for the top, bridge and hollow sites, respectively, at 0.25 ML coverage. Thus, we may deduce from these similar and related works [18,91] that when an alkali metal (i.e., K, Na, and Li) is adsorbed on an fcc (100) surface, the hollow site is the energetically preferred adsorption site, as confirmed in the present work. We note however that our GGA–PBE calculations on Li/Ag(100) system predict higher adsorption energy values with respect to those obtained on Li/Pt(100) or K/Fe(100) system. Also, as shown in Table 4, the values of the structural parameters as obtained with the PBE+d3 functional are similar to those calculated with GGA–PBE calculations. Finally, similarly to the case of d_{H-Ag} case, the distances d_{Li-Ag} increase when the coordination number around the adsorbate (Li or H) increases.

3.3.2. *Work function change and dipole moment due to Li adsorption on Ag(100) surface*

Our results show that the adsorption of Li atom on Ag surface decreases the work function of clean Ag(100) surface, giving a negative value of work function change. Similarly, Kiskinova et al. [92] have found that K adsorbed on Pt(111) surface strongly decreases the work function from the value of the clean Pt(111) surface. Then, Li, Na and K work function change calculations on Co(0001) surface also showed a decreases [93]. The finding by Saad et al. [18] and Mannstadt [58] who found negative values of work function change when Li adsorbed on Pt and Ru surfaces, respectively, are also consistent with our results. Similar to the case of H adsorption on Ag(100), the adsorption of Li on Ag(100) results in structural changes to the surface and attendant electron redistribution which impacts on the work function of the surface and thus, the observed negative work function change. Furthermore, we also note that in all coverages, the $\Delta\Phi$ change depends on the adsorption site such that there is an appreciable change as the coverage increases in the cases of Li adsorption on the top and hollow sites. However, the change in the $\Delta\Phi$ is less pronounced for the hollow site. In addition, we observed that the GGA–PBE functional has more significant effect on the $\Delta\Phi$ compared to the PBE+d3 functional. Also, in all the possible adsorption sites, the lowest dipole moment are located at 0.25 ML while the highest values are at 1.00 ML coverages. The negative value of the dipole moment suggest that the Li-Ag dipole is orientated toward adsorbate.

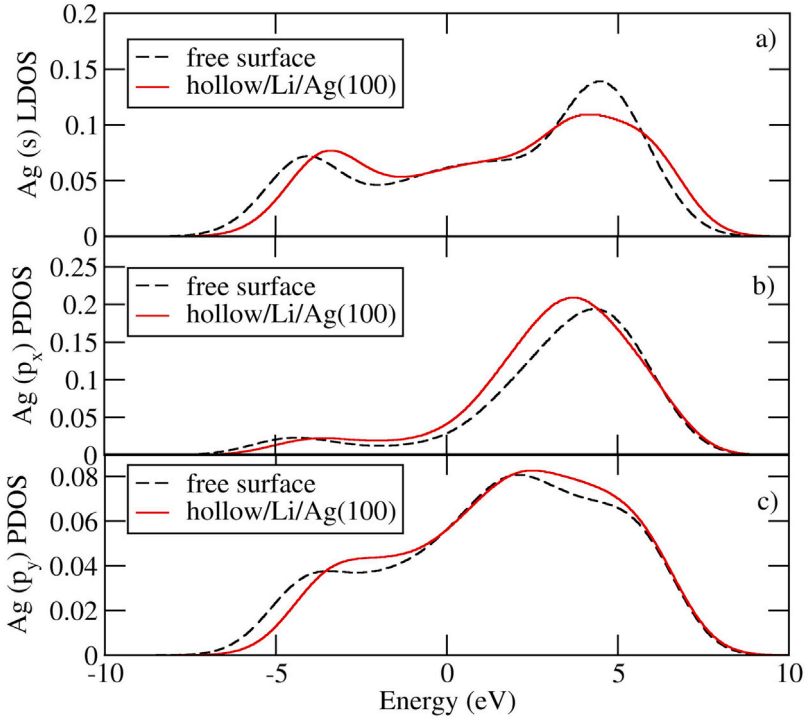

Fig. 7. (Color online) LDOS *s* and PDOS p_x and p_y of Ag bands after Li adsorption on Ag(100) surface and LDOS *s* and PDOS p_x and p_y of Ag bands of the bare surface. The zero energy denotes the Fermi level.

Table 5
Coadsorption energies of H and Li (E_{coads}), coadsorption energies of H (E^{H}_{coads}), coadsorption energies of Li (E^{Li}_{coads}) and structural parameters (d_{H-Li}, d_{H-Ag} and d_{Li-Ag}) of (H+Li)/Ag(100) for several configurations. The values obtained with PBE calculations are outside parentheses and in the parenthesis are listed the results with PBE+d3.

Calculated parameters	Configurations				
	Li(h)+ H(t)	Li(h)+ H(b1)	Li(h)+ H(b2)	Li(h)+ H(h1)	Li(h)+ H(h2)
E_{coads} (eV)	−5.29 (−5.49)	−5.391 (−5.56)	−5.18 (−5.41)	−5.04 (−5.30)	−5.09 (−5.34)
E^{H}_{coads} (eV)	−3.11 (−3.12)	−3.21 (−3.23)	−3.01 (−3.05)	−2.86 (−2.93)	−2.92 (−2.98)
E^{Li}_{coads} (eV)	−2.80 (−2.93)	−2.47 (−2.62)	−2.26 (−2.44)	−2.16 (−2.34)	−2.21 (−2.38)
d_{H-Li} (Å)	1.86 (1.90)	1.86 (1.91)	3.32 (3.26)	3.20 (3.14)	4.40 (4.32)
d_{H-Ag} (Å)	1.92 (1.94)	1.85 (1.88)	2.16 (2.20)	2.11 (2.13)	1.77 (1.79)
d_{Li-Ag} (Å)	2.80 (2.84)	2.72 (2.76)	2.77 (2.80)	2.75 (2.79)	2.71 (2.73)
$\Delta\Phi$ (eV)	−0.02 (−0.10)	−0.29 (−0.32)	−0.31 (−0.34)	−0.32 (−0.34)	−0.29 (−0.32)
$\Delta\mu$ (Debye)	−0.02 (−0.09)	−0.27 (−0.28)	−0.29 (−0.31)	−0.29 (−0.31)	−0.27 (−0.29)

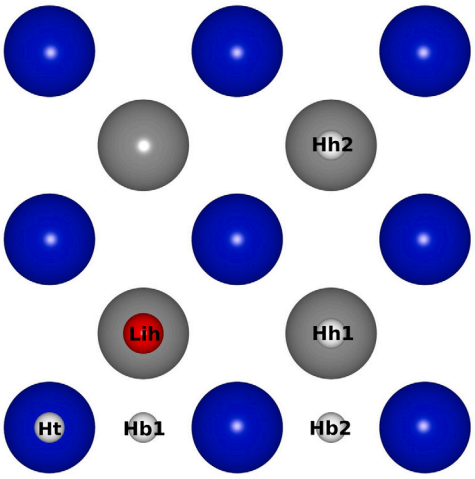

Fig. 8. Coadsorption sites of Li and H on Ag (100) surface: **Ht**, H on top site with one nearest Li neighbor atom; **Hb1**, H on bridge site with one nearest neighbor of Li; **Hb2**, H on bridge site with two next-nearest Li neighbors; **Hh1**, H on hollow site with two second-nearest Li neighbors; **Hh2**, H on hollow site with four second nearest Li neighbors. Li is shown at the most stable site (hollow site). In blue and gray the Ag atoms of the surface and subsurface, respectively. (For interpretation of the references to color in this figure legend, the reader is referred to the web version of this article.)

3.3.3. Local (Projected) Density of States (L(P)DOS)

Similar to the case of the adsorption of H on Ag(100) surface, we analyze the electronic bonding in Li adsorbed on Ag(100) using the LDOS and PDOS of Li adsorbed on the most stable site (hollow) at the 0.25 ML coverage. This is shown in Fig. 6 for the Li s LDOS upon the adsorption of Li on Ag(100) surface. The LDOS of free Li is also shown for comparison. The adsorption of Li on Ag(100) changes the occupation of s state when compared to the free Li, as indicated by the shift of LDOS toward higher energies (above the Fermi level). The shift in the peak above the Fermi level suggest that Li has transferred its s electrons to the Ag surface. Also, we observe a decrease in the peak intensity of Li LDOS after the adsorption. The shift and the reduction in the peak of Li LDOS upon adsorption result from mixture or hybridization between the Li and Ag bands. Also, in Fig. 7 the s, p_x and p_y bands of the Ag atom when Li atom is adsorbed on the Ag(100) surface is shown. The bare surface bands are also shown for comparison. There is a small relative shift toward the higher energies for the s, p_x and p_y bands, in particular at the occupied energy levels below the Fermi level. This suggests strong interaction between Li and the Ag surface.

Also, we notice decrease in the peak of s band peaks situated at about 4.51 eV. Meanwhile, an increase in the peak intensity of s (−4.11 eV), p_x (4.34 eV) and p_y (2.14 eV) bands is observed. These modifications in the electronic structure can be associated to hybridization between Li and Ag bands.

3.4. Coadsorption of H and Li on Ag(100) surface

3.4.1. Coadsorption energies and structural parameters

Having discussed the adsorption of each of H and Li on the Ag(100) surface, here we focus on coadsorption of H and Li on Ag(100) surface. We have explored the coadsorption of H and Li on Ag(100) by considering five combinations using a (2 × 2) unit cell and a coverage of 0.25 ML. In our study, we have fixed Li on the only stable hollow site while the position of the H is varied as shown in Fig. 8. Five different combinations of H-Li on Ag(100) is shown. These can be described as follows: in **Ht**, there is H on top site with one nearest Li neighbor atom; in **Hb1**, H is on bridge site with one nearest neighbor of Li; in **Hb2**, H is on bridge site with two next-nearest Li neighbors; also in **Hh1**, the H is on the hollow site with two second-nearest Li neighbors; in **Hh2**, H is on the hollow site with four second nearest Li neighbors. Li is shown at the most stable site (hollow site).

Data concerning the coadsorption of H and Li on Ag(100) are presented in the Table 5. Our calculations shows that, the coadsorption of H and Li is favorable on Ag(100) surface for all the five possible combinations as investigated. The Li-H coadsorption energy is in excess of −5 eV. We found that for the bridge configurations where the H is at either the $b1$ and $b2$ sites, i.e., Li(h)+ H(b1) and Li(h)+ H(b2) (Fig. 8) combinations, the more favorable Li-H combination is where the H is closest to Li atom, i.e., Li(h)+ H(b1). This is in contrast to the work of Saad et al. [18] who have reported this configuration to be less stable by citing possible electronic repulsion between the Li and H atoms at such a close separation. In the case of hollow coadsorption sites Li(h)+H(h1) and Li(h)+H(h2), we find that the more stable configuration is the latter, that is, where H is located at the greater distance from Li, in agreement with Saad et al. [18]. Furthermore, Table 5 shows that the most stable configuration of all configurations is the Li(h)+ H(b1), with the coadsorption energy of −5.39 eV (−5.56 eV) where the relaxed configuration shows that H is located at 3.32 Å (3.32 Å) from Li, for the GGA–PBE (PBE+d3) functionals. In addition, the stability order of H and Li coadsorption on Ag(100) surface is: Li(h)+ H(b1) > Li(h)+ H(t) > Li(h)+ H(b2) > Li(h)+H(h2) > Li(h)+H(h1).

In addition, the results of coadsorption energies of H listed in Table 5 affirms the bridge site to be the most preferred site even when H is coadsorbed with Li, as shown by the E_{coads} of Li(h)+ H(b1) and the coadsorption energy of H (E^{H}_{coads}). This is consistent with the previous study [18] which reported that after the adsorption of Li, the bridge site remain the preferred adsorption site of H. In actual fact, in all the Li-H coadsorption, the H at the bridge site, $b1$, is most favorable, however H at the t site is more preferred site when compared to the bridge site, $b2$. We may summarize the trend in H coadsorption with Li on the Ag(100) as follows: bridge site $b1$ > top site t > bridge site $b2$ > hollow site $h2$ > hollow site $h1$. We should also note that when the E^{H}_{coads} (Table 5) is compared with E_{ads} of H in Table 3, one may deduce that the co-presence of Li at the hollow site with the H at the bridge site actually increases the adsorption energy of the latter to the Ag(100) surface, since the E^{H}_{coads} is slightly more negative (i.e., about

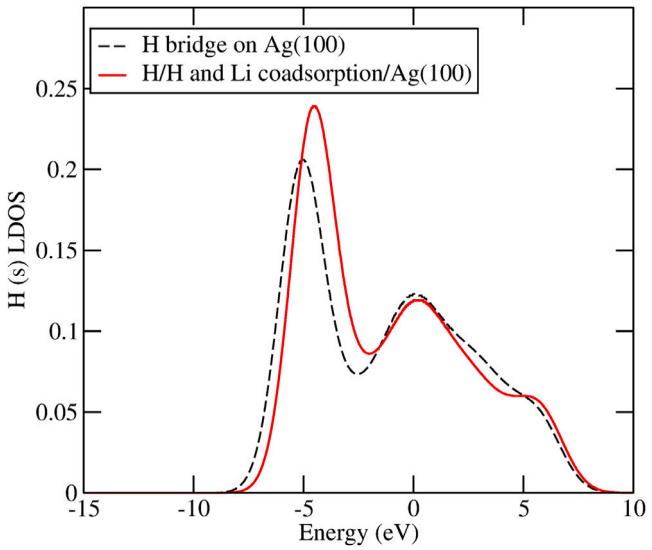

Fig. 9. (Color online) LDOS of s orbital of H after H and Li coadsorption on Ag(100) surface and LDOS of adsorbed H on Ag(100). The zero energy corresponds to value the Fermi level.

−3.21, Table 5) compared to E_{ads} of H to the bare Ag(100) surface, of about −2.92 eV (Table 3). Similarly, we find that Li adsorption is enhanced with coadsorption with H. This is clearly seen when Table 4 is compared with Table 5. It will be seen that the co-presence of H at the hollow ($h1$) site with the Li at the hollow site actually increases the adsorption energy of the latter to the Ag(100) surface, since the E^{Li}_{coads} is also slightly more negative (i.e., about −2.47 (−2.62), PBE (PBE + d3), respectively; Table 5) compared to the E_{ads} of Li to the bare Ag (100) surface, of about −2.20 eV (−2.37 eV) for the PBE (PBE+d3) as shown in Table 3. Finally, we remark that the distances $d_{\mathrm{H-Ag}}$ and $d_{\mathrm{Li-Ag}}$ as calculated in the coadsorption study of H-Li on Ag (100) are similar to those evaluated for each of H (Section 3.2) and Li (Section 3.3) adsorptions.

3.4.2. Work function change and dipole moment of Ag(100) surface

The calculated work function changes are in the following order: Li(h)+H(h1) < Li(h)+H(b2) < Li(h)+H(b1) < Li(h)+H(h1) < Li(h)+H(t). Generally, in all the configurations, the work function change is negative, meaning that the work function is lowered when the Li-H is adsorbed on the Ag(100) surface. To this end, we note that when Li and H are adsorbed on the Ag(100) surface, there is a redistribution of the electronic density at the surface. The decrease in the work function may be explained as due to the smoothing of the modulation of the electronic density of the surface. It is well known that alkali-atom in particular such as Li, when adsorbed on metals lose part of their valence charge to the metal substrate. Also, when hydrogen is adsorbed on metals, its structural influence on the metal surface is accompanied by a redistribution of electronic charges within the surface leading to unexpected or unforeseen changes of the electronic work function. We may therefore conclude that combined structural influence and electronic charge redistribution are responsible for the decrease in the work function when Li and H are co-adsorbed on the Ag(100) surface. The decrease in the work function with Li and H coadsorption suggests possible transfer of electron from the Li-H adsorbates to the Ag(100) surface. Also, the change in the work function after Li-H coadsorption induces a surface dipole moment, which in turn affects the work function. Table 5 shows that: $\Delta\mu_{\mathrm{Li}(h)+\mathrm{H}(h1)} < \Delta\mu_{\mathrm{Li}(h)+\mathrm{H}(b2)} < \Delta\mu_{\mathrm{Li}(h)+\mathrm{H}(b1)} < \Delta\mu_{\mathrm{Li}(h)+\mathrm{H}(h1)} < \Delta\mu_{\mathrm{Li}(h)+\mathrm{H}(t)}$. We this conclude that the (H+Li)-Ag dipole points toward adsorbates.

3.4.3. Local Density of States (LDOS)

Here, we analyze the evolution of LDOS of H, Li and Ag atoms in the H-Li on Ag(100) surface system. We limit our discussion to the most stable configuration, of Li(h)+H(b1). Fig. 9 shows the H s LDOS when H and Li are coadsorbed on Ag(100) surface. Also, the H s LDOS for adsorbed H is presented.

An increase and a slight shift toward higher energies of peak located at −5.01 eV of H is observed when H is coadsorbed on Ag(100).

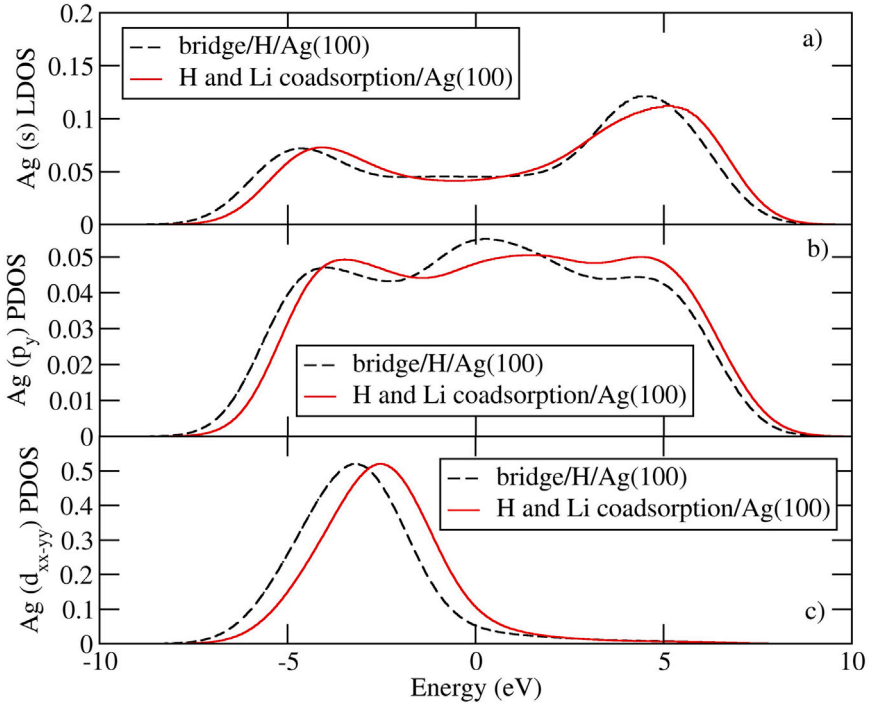

Fig. 10. (Color online) LDOS s and PDOS p_y and d_{xx-yy} of Ag bands after H and Li adsorption on Ag(100) surface and LDOS s and PDOS p_y and d_{xx-yy} of Ag bands after H adsorption on Ag(100) surface. The zero energy corresponds to the Fermi level.

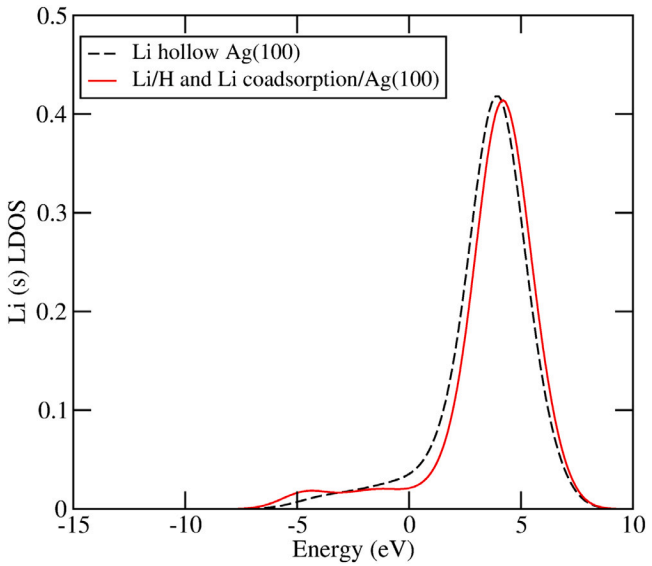

Fig. 11. (Color online) LDOS of s orbital of Li after coadsorption of H and Li on Ag(100) surface and LDOS of adsorbed Li on Ag(100). The zero energy denotes the Fermi level.

However, for the peak located at −0.12 eV, there is only a slight decrease in the peak intensity. In general, the peaks are qualitatively similar.

Fig. 10 shows decomposition of s, p_y and d_{xx-yy} bands of Ag surface atom in Li(h)+H(b1). The same bands when only H is adsorbed on Ag(100) are also presented for comparison.

A slight displacement of s, p_y and d_{xx-yy} bands of Ag toward higher energies is observed in particular for the Ag s band. For the p_y and d_{xx-yy} bands, the shift in the peaks is more pronounced at lower energy, below the Fermi level. Concerning the s band (Fig. 10(a)), the peak located below the Fermi level in both adsorption of H and coadsorption with Li on Ag, have the same intensity. For the Ag d_{xx-yy} band, the single pronounced peak is only displaced toward the higher energies, but yet below the Fermi level (Fig. 10(c)).

In Fig. 11, the Li s LDOS when H and Li are co-adsorbed on Ag(100) surface is presented. The Li s LDOS when only Li is adsorbed on Ag(100) surface is presented. The Fig. 11 shows that: (i) the most intense peak is located above the Fermi level, i.e, the domain of the unoccupied states; (ii) at the Fermi level, the Li(s) LDOS without H has a DOs of 0.03 e^-. After coadsorption of H and Li, the Li(s) LDOS at the Fermi level reduced to 0.02 e^-.

Fig. 12 shows the evolution of s, p_x and p_y bands of Ag surface atom in Li(h)+H(b1) configuration. The s, p_x and p_y bands of Ag in Li adsorption on Ag(100) are also presented for a comparison. Here, the LDOSs shows a slight displacement toward lower energy when the H and Li are coadsorbed, in particular for the peak located below the Fermi level. This is clearly evident for the Ag (s) peak (Fig. 10(a)) and Ag(p_y) (Fig. 10(b)). However, a slight shift of the Ag (s) toward the higher energies for the broad peak located above the Fermi level is observed. The most noticable change in the Ag(p_x) and Ag(p_y), in Fig. 12(b & c) respectively, is the significant change in the intensity of the peaks due to coadsorption even though the peaks are qualitatively similar. There is a pronounced decrease in the peak intensity above the Fermi level for the Ag(p_x) when H and Li are coadsorbed on the Ag(100) surface (Fig. 12(b)). For the Ag(p_y), there is an increase in the peak intensity below for the peak below the Fermi level and a decrease in the intensity of the peak level above the Fermi level (Fig. 12(c)). The shifts in the energy positions of the LDOS along with increase or reduction in the peak intensity when Li and H are coadsorbed on the Ag (100) surface are indicative of electronic interactions between Ag, Li and H atoms. Finally, when the energy positions of the peaks are considered for the orbitals of Li, H and Ag, one will notice a strong hybridization between the orbitals, in particular between −5 eV to + 5 eV. This hybridization is responsible for the stability of the Li(h)+H(b1) configuration.

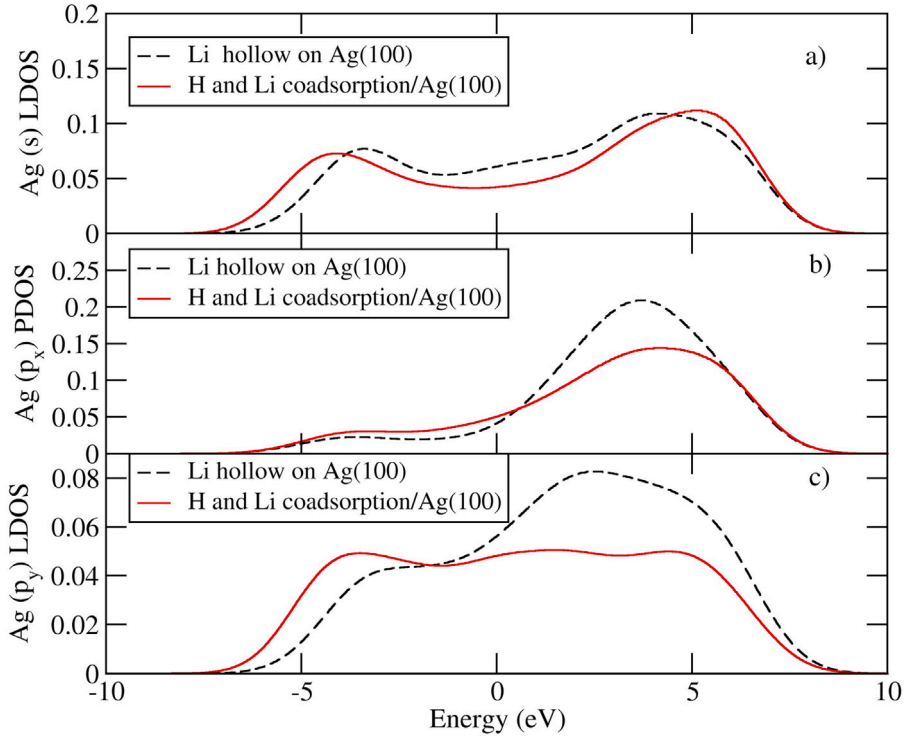

Fig. 12. (Color online) LDOS s and PDOS p_x and p_y of Ag band after H and Li adsorption on Ag(100) surface and LDOS s and PDOS p_x and p_y of Ag band after Li adsorption on Ag(100) surface. The zero energy denotes the Fermi level.

4. Conclusion

Density functional theory (DFT) calculations using the GGA–PBE and DFT+d3 dispersion correction have been performed to study the adsorption of H and Li as well as their coadsorption on Ag(100) surface. As a benchmark calculations, we obtain structural and electronic properties of bulk and clean Ag (100) surface. We found good agreement with previous DFT studies as well as available experimental data. Also, we obtain the adsorption energies, coadsorption energies, structural relaxation parameters, work function change and dipole moment for the adsorption and coadsorption of Li, H and Li+H adsorbates on the Ag(100) surface. These parameters are obtained as a function of adsorbate coverage on the Ag(100) surface. Our GGA–PBE calculations show that H when adsorbed on the Ag(100) surface prefers the bridge site at 0.25 and 0.50 ML coverages and hollow site at the 0.75 and 1.00 ML coverages. For DFT+d3 calculations, we find that H is most stable at bridge site at the 0.25 ML coverage, however, it prefers the hollow site at the 0.50, 0.75 and 1.00 ML coverages. In the case of Li adsorption on Ag(100) surface, both GGA–PBE and DFT+d3 calculations suggest that Li is most stable at hollow site. We then considered five configurations of H and Li coadsorption on Ag(100) surface at 0.25ML adsorbate coverage, for which we find the Li at the hollow site with H at the nearest-neighbor bridge site configurations as the most energetically favorable structure. Our electronic structure calculations show shifts in the energy levels, reduction or increase in the density of states peaks of Li, H and Ag. Also, the energy positions of the various peaks shows strong hybridization between the orbitals and hence the stability of this configuration. Furthermore, we observed a decrease in the work function when Li is adsorbed on the Ag(100) surface. Similar observation was made when Li-H are coadsorbed on the Ag(100). We adduced this decrease to redistribution of the electronic density at the surface due to the Li and Li-H adsorbates. The change in the work function induces surface dipole moment change. The results obtained for the dipole moment change shows that the influence of Li dominates the behavior of the Li-H/Ag(100) system, producing an electron transfer from adsorbate to substrate, as it was obtained for the Li/Ag(100) system.

Declaration of competing interest

The authors declare that they have no known competing financial interests or personal relationships that could have appeared to influence the work reported in this paper.

Acknowledgments

The computational resources are provided by the Center for High Performance Computing (CHPC), Cape Town, South Africa through the MATS0988 project.

References

[1] T. Jacob, The mechanism of forming H_2O from H_2 and O_2 over a Pt catalyst via direct oxygen reduction, Fuel Cells 6 (3–4) (2006) 159–181.
[2] M.T.M. Koper, R.A. van Santen, Interaction of H, O and OH with metal surfaces, J. Electroanal. Soc. 472 (2) (1999) 126–136.
[3] A. Eichler, J. Hafner, G. Kresse, Hydrogen adsorption on the (100) surfaces of rhodium, palladium and silver, Surf. Rev. Lett. 4 (06) (1997) 1297–1303.
[4] C. Qin, J.L. Whitten, Adsorption of O, H, OH, and H_2O on Ag(100), J. Phys. Chem. B 109 (18) (2005) 8852–8856.
[5] S.C. Jung, M.H. Kang, Effect of hydrogen on the surface relaxation of Pd(100), Rh(100), and Ag(100), Phys. Rev. B 72 (20) (2005) 205419–205425.
[6] P. Ferrin, S. Kandoi, A.U. Nilekar, M. Mavrikakis, Hydrogen adsorption, absorption and diffusion on and in transition metal surfaces: A DFT study, Surf. Sci. 606 (7–8) (2012) 679–689.
[7] E.V. Gómez, S. Amaya-Roncancio, L.B. Avalle, D.H. Linares, M.C. Gimenez, DFT study of adsorption and diffusion of atomic hydrogen on metal surfaces, Appl. Surf. Sci. 420 (2017) 1–8.
[8] F.O. Sanchez-Varretti, E.V. Gómez, L.B. Avalle, F.M. Bulnes, M.C. Gimenez, A.J. Ramirez-Pastor, Monte Carlo Simulations and cluster-exact approximation applied to H/Cu(100), H/Ag(100) and O/Cu(100) systems, Appl. Surf. Sci. 500 (2020) 144034–144056.
[9] B.W.J. Chen, D. Kirvassilis, Y. Bai, M. Mavrikakis, Atomic and molecular adsorption on Ag(111), J. Phys. Chem. C 123 (13) (2018) 7551–7566.
[10] A. Montoya, A. Schlunke, B.S. Haynes, Reaction of hydrogen with Ag(111): Binding states, minimum energy paths, and kinetics, J. Phys. Chem. B 110 (34) (2006) 17145–17154.
[11] M. N'dollo, P.S. Moussounda, T. Dintzer, F. Garin, A density functional theory study of methoxy and atomic hydrogen chemisorption on Au(100) surface, J. Mod. Phys. 4 (1) (2013) 409–417.
[12] Y. Santiago-Rodriguez, J.A. Herron, M.C. Curet-Arana, M. Mavrikakis, Atomic and molecular adsorption on Au(111), Surf. Sci. 627 (2014) 57–69.
[13] M. Mavrikakis, J. Rempel, J. Greeley, L.B. Hansen, J.K. Nørskov, Atomic and molecular adsorption on Rh(111), J. Chem. Phys. 117 (14) (2002) 6737–6744.
[14] S. Wilke, V. Natoli, M.H. Cohen, Theoretical investigation of water formation on Rh and Pt surfaces, J. Chem. Phys. 112 (22) (2000) 9986–9995.
[15] J.A. Herron, S. Tonelli, M. Mavrikakis, Atomic and molecular adsorption on Pd(111), Surf. Sci. 606 (21–22) (2012) 1670–1679.
[16] G.W. Watson, R.P.K. Wells, D.J. Willock, G.J. Hutchings, A comparison of the adsorption and diffusion of hydrogen on the {111} surfaces of Ni, Pd, and Pt from density functional theory calculations, J. Phys. Chem. B 105 (21) (2001) 4889–4894.
[17] P.S. Moussounda, M.F. Haroun, G. Rakotovelo, P. Légaré, A theoretical study of CH_4 dissociation on Pt(100) surface, Surf. Sci. 601 (18) (2007) 3697–3701.
[18] F. Saad, M. Zemirli, M. Benakki, S. Bouarab, Ab-initio study of the coadsorption of Li and H on Pt (001), Pt (110) and Pt (111) surfaces, Physica B 407 (4) (2012) 698–704.
[19] C.D. Vurdu, The adsorption and diffusion manners of hydrogen atoms on Pt(100), Pt(110), and Pt(111) surfaces, Adv. Condens. Matter Phys. 2018 (2018) 1–10.
[20] D.C. Ford, Y. Xu, M. Mavrikakis, Atomic and molecular adsorption on Pt(111), Surf. Sci. 587 (3) (2005) 159–174.
[21] L. Xu, J. Lin, Y. Bai, M. Mavrikakis, Atomic and molecular adsorption on Cu(111), Top. Catalysis 61 (9–11) (2018) 736–750.
[22] K. Gundersen, B. Hammer, K.W. Jacobsen, J.K. Nørskov, J.S. Lin, V. Milman, Chemisorption and vibration of hydrogen on Cu(111), Surf. Sci. 285 (1–2) (1993) 27–30.
[23] J. Strömquist, L. Bengtsson, M. Persson, B. Hammer, The dynamics of h absorption in and adsorption on Cu(111), Surf. Sci. 397 (1–3) (1998) 382–394.
[24] E.V. Gómez, L.B. Avalle, M.C. Gimenez, A first-principle study of h adsorption and absorption under the influence of coverage, Int. J. Hydrogen Energy 44 (2019) 7083–7094.
[25] Y. Bai, D. Kirvassilis, L. Xu, M. Mavrikakis, Atomic and molecular adsorption on Ni(111), Surf. Sci. 679 (2019) 240–253.
[26] J. Greeley, M. Mavrikakis, A first-principles study of surface and subsurface H on and in Ni(111): diffusional properties and coverage-dependent behavior, Surf. Sci. 540 (2–3) (2003) 215–229.
[27] K. Hahn, M. Mavrikakis, Atomic and molecular adsorption on Re(0001), Top. Catalysis 57 (1–4) (2014) 54–68.
[28] J.A. Herron, S. Tonelli, M. Mavrikakis, Atomic and molecular adsorption on Ru(0001), Surf. Sci. 614 (2013) 64–74.
[29] L. Xu, D. Kirvassilis, Y. Bai, M. Mavrikakis, Atomic and molecular adsorption on Fe(110), Surf. Sci. 667 (2018) 54–65.
[30] D.E. Jiang, E.A. Carter, Adsorption and diffusion energetics of hydrogen atoms on Fe(110) from first principles, Surf. Sci. 547 (1–2) (2003) 85–98.
[31] A. Juan, R. Hoffmann, Hydrogen on the Fe(110) surface and near bulk bcc Fe vacancies: a comparative bonding study, Surf. Sci. 421 (1–2) (1999) 1–16.
[32] W.P. Krekelberg, J. Greeley, M. Mavrikakis, Atomic and molecular adsorption on Ir(111), J. Phys. Chem. B 108 (3) (2004) 987–994.
[33] P. Matczak, S. Romanowski, The effect of alloying on the H-atom adsorption on the (100) surfaces of Pd-Ag, Pd-Pt, Pd-Au, Pt-Ag, and Pt-Au. A theoretical study, Cent. Eur. J. Chem. 9 (3) (2011) 474–480.
[34] G. Lee, P.T. Sprunger, M. Okada, D.B. Poker, D.M. Zehner, E.W. Plummer, Chemisorption of hydrogen on the Ag(111) surface, J. Vac. Sci. Technol. A: Vac. Surf. Films 12 (4) (1994) 2119–2123.
[35] G. Lee, E.W. Plummer, Interaction of hydrogen with the Ag(111) surface, Phys. Rev. B 51 (11) (1995) 7250–7261.
[36] L. Hammer, H. Landskron, W. Nichtl-Pecher, A. Fricke, K. Heinz, K. Müller, Hydrogen-induced restructuring of close-packed metal surfaces: H/Ni(111) and H/Fe(110), Phys. Rev. B 47 (23) (1993) 15969–15972.
[37] V. Ledentu, W. Dong, P. Sautet, Heterogeneous catalysis through subsurface sites, J. Am. Chem. Soc. 122 (8) (2000) 1796–1801.
[38] H. Okuyama, T. Ueda, T. Aruga, M. Nishijima, Overtones of H vibrations at Ni(111): Formation of delocalized states, Phys. Rev. B 63 (23) (2001) 233403–233404.
[39] K.J. Maynard, A.D. Johnson, S.P. Daley, S.T. Ceyer, A new mechanism for absorption: collision-induced absorption, Faraday Discuss. Chem. Soc. 91 (1991) 437–449.

[40] W. Nichtl-Pecher, J. Gossmann, L. Hammer, K. Heinz, K. Müller, Adsorption of hydrogen on Fe(110) at cryogenic temperatures investigated by low energy electron diffraction, J. Vac. Sci. Technol. A: Vac. Surf. Films 10 (3) (1992) 501–507.

[41] W. Moritz, R. Imbihl, R.J. Behm, G. Ertl, T. Matsushima, Adsorption geometry of hydrogen on Fe(110), J. Chem. Phys. 83 (4) (1985) 1959–1968.

[42] E.A. Kurz, J.B. Hudson, The adsorption of H_2 and D_2 on Fe(110): II. Angle resolved thermal desorption spectroscopy and kinetic mechanism, Surf. Sci. 195 (1–2) (1988) 31–42.

[43] T. Mitsui, M.K. Rose, E. Fomin, D.F. Ogletree, M. Salmeron, Hydrogen adsorption and diffusion on Pd(111), Surf. Sci. 540 (1) (2003) 5–11.

[44] L.C. Fernández-Torres, E.C.H. Sykes, S.U. Nanayakkara, P.S. Weiss, Dynamics and spectroscopy of hydrogen atoms on Pd {111}, J. Phys. Chem. B 110 (14) (2006) 7380–7384.

[45] T. Mitsui, M.K. Rose, E. Fomin, D.F. Ogletree, M. Salmeron, Dissociative hydrogen adsorption on palladium requires aggregates of three or more vacancies, Nature 422 (6933) (2003) 705–707.

[46] T. Mitsui, E. Fomin, D.F. Ogletree, M. Salmeron, A.U. Nilekar, M. Mavrikakis, Manipulation and patterning of the surface hydrogen concentration on pd(111) by electric fields, Angew. Chem. Int. Ed. 46 (30) (2007) 5757–5761.

[47] L.J. Richter, W. Ho, Vibrational spectroscopy of H on Pt(111): Evidence for universally soft parallel modes, Phys. Rev. B 36 (18) (1987) 9797.

[48] Ş. Bădescu, P. Salo, T. Ala-Nissila, S.-C. Ying, K. Jacobi, Y. Wang, K. Bedürftig, G. Ertl, Energetics and vibrational states for hydrogen on Pt(111), Phys. Rev. Lett. 88 (13) (2002) 136101–136104.

[49] H. Conrad, R. Scala, W. Stenzel, R. Unwin, Adsorption of hydrogen HREELS and deuterium on Ru(001), J. Chem. Phys. 81 (12) (1984) 6371–6378.

[50] G. Lee, D.B. Poker, D.M. Zehner, E.W. Plummer, Coverage and structure of deuterium on Cu(111), Surf. Sci. 357 (1996) 717–720.

[51] G. Lee, E.W. Plummer, High-resolution electron energy loss spectroscopy study on chemisorption of hydrogen on Cu(111), Surf. Sci. 498 (3) (2002) 229–236.

[52] C.L.A. Lamont, B.N.J. Persson, G.P. Williams, Dynamics of atomic adsorbates: hydrogen on Cu(111), Chem. Phys. Lett. 243 (5–6) (1995) 429–434.

[53] I.G. Shuttleworth, Analysis of the (3× 3)-H/Cu(111) system using eikonal-level helium atom scattering simulations, Surf. Rev. Lett. 14 (06) (2007) 1089–1093.

[54] J.T. Yates Jr, P.A. Thiel, W.H. Weinberg, The chemisorption of hydrogen on Rh(111), Surf. Sci. 84 (2) (1979) 427–439.

[55] C.J. Hagedorn, M.J. Weiss, W.H. Weinberg, Dissociative chemisorption of hydrogen on Ir(111): Evidence for terminal site adsorption, Phys. Rev. B 60 (20) (1999) R14016.

[56] J. Lauterbach, M. Schick, W.H. Weinberg, Coadsorption of CO and hydrogen on the Ir(111) surface, J. Vac. Sci. Technol. A: Vac. Surf. Films 14 (3) (1996) 1511–1515.

[57] I. Ohsaki, T. Oguchi, Theoretical study of STM in Cu(001)-(2× 1)–Li, Surf. Sci. 438 (1–3) (1999) 26–30.

[58] W. Mannstadt, Coverage dependence of the work function of Li adsorbed on Ru(001): ab initio studies within DFT, Surf. Sci. 525 (1–3) (2003) 119–125.

[59] H. Jiang, M. Imaki, S. Mizuno, H. Tochihara, (N× n) surface structures formed commonly on Cu(001), Ag(001) and Ni(001) by alkali-metal adsorption, Surf. Rev. Lett. 4 (06) (1997) 1227–1232.

[60] B.E. Hayden, K.C. Prince, P.J. Davie, G. Paolucci, A.M. Bradshaw, Alkali metal-induced reconstruction of Ag(110), Solid State Commun. 48 (4) (1983) 325–328.

[61] S.D. Parker, Lithium adsorption on Ag(111): Characterization by AES and work function changes, Surf. Sci. 157 (2–3) (1985) 261–272.

[62] A. Mikkelsen, J.H. Petersen, S.V. Hoffmann, J. Jiruse, D.L. Adams, Structure and formation of surface alloys by adsorption of Li on Al(110), Surf. Sci. 487 (1–3) (2001) 28–38.

[63] P. Giannozzi, S. Baroni, N. Bonini, M. Calandra, R. Car, C. Cavazzoni, D. Ceresoli, G.L. Chiarotti, M. Cococcioni, I. Dabo, et al., QUANTUM ESPRESSO: a modular and open-source software project for quantum simulations of materials, J. Phys.: Condens. Matter 21 (39) (2009) 395502–395520.

[64] J.P. Perdew, K. Burke, M. Ernzerhof, Generalized gradient approximation made simple, Phys. Rev. Lett. 77 (18) (1996) 3865.

[65] S. Grimme, J. Antony, S. Ehrlich, H. Krieg, A consistent and accurate ab initio parametrization of density functional dispersion correction (DFT-D) for the 94 elements H-Pu, J. Chem. Phys. 132 (15) (2010) 154104–154119.

[66] M.P.A.T. Methfessel, A.T. Paxton, High-precision sampling for brillouin-zone integration in metals, Phys. Rev. B 40 (6) (1989) 3616–3621.

[67] F.D. Murnaghan, The compressibility of media under extreme pressures, Proc. Natl. Acad. Sci. USA 30 (9) (1944) 244–247.

[68] C.C. Boungou, M. N'dollo, B.R. Malonda-Boungou, P.S. Moussounda, T. Dintzer, Theoretical simulation of isocyanate (NCO) adsorption on the Ag(001) surface, J. Korean Phys. Soc. 68 (10) (2016) 1192–1199.

[69] A. Ambrosetti, P.L. Silvestrelli, Cohesive properties of noble metals by van der Waals–corrected density functional theory: Au, Ag, and Cu as case studies, Phys. Rev. B 94 (4) (2016) 045124–045133.

[70] J. Avelar, A. Bruix, J. Garza, R. Vargas, Van der Waals exchange-correlation functionals over bulk and surface properties of transition metals, J. Phys.: Condens. Matter 31 (31) (2019) 315501–315519.

[71] A. Migani, C. Sousa, F. Illas, Chemisorption of atomic chlorine on metal surfaces and the interpretation of the induced work function changes, Surf. Sci. 574 (2–3) (2005) 297–305.

[72] G. Cipriani, D. Loffreda, A. Dal Corso, S. de Gironcoli, S. Baroni, Adsorption of atomic oxygen on Ag(001): a study based on density-functional theory, Surf. Sci. 501 (3) (2002) 182–190.

[73] B. He, D. Ma, W. Hao, W. Xiao, Z. Tian, Ag(100)/MgO(100) interface: A van der Waals density functional study, Appl. Surf. Sci. 288 (2014) 115–121.

[74] P. Janthon, S.M. Kozlov, F. Vines, J. Limtrakul, F. Illas, Establishing the accuracy of broadly used density functionals in describing bulk properties of transition metals, J. Chem. Theory Comput. 9 (3) (2013) 1631–1640.

[75] C. Kittel, Int. to Solid State Physics, Maruzen, 2005.

[76] K. Lejaeghere, V. Van Speybroeck, G. Van Oost, S. Cottenier, Error estimates for solid-state density-functional theory predictions: an overview by means of the ground-state elemental crystals, Crit. Rev. Solid State Mater. Sci. 39 (1) (2014) 1–24.

[77] M. Chelvayohan, C.H.B. Mee, Work function measurements on (110), (100) and (111) surfaces of silver, J. Phys. C: Solid State Phys. 15 (10) (1982) 2305–2312.

[78] J. Wang, S.-Q. Wang, Surface energy and work function of fcc and bcc crystals: Density functional study, Surf. Sci. 630 (2014) 216–224.

[79] H. Fu, L. Jia, W. Wang, K. Fan, The first-principle study on chlorine-modified silver surfaces, Surf. Sci. 584 (2–3) (2005) 187–198.

[80] M.G. Stachiotti, First-principles study of the adsorption of NH_3 on Ag surfaces, Phys. Rev. B 79 (11) (2009) 115405–115409.

[81] W.R. Tyson, W.A. Miller, Surface free energies of solid metals: Estimation from liquid surface tension measurements, Surf. Sci. 62 (1) (1977) 267–276.

[82] H. Li, J. Quinn, Y.S. Li, D. Tian, F. Jona, P.M. Marcus, Multilayer relaxation of clean Ag{001}, Phys. Rev. B 43 (9) (1991) 7305–7307.

[83] H.L. Davis, J.R. Noonan, Multilayer relaxation in metallic surfaces as demonstrated by LEED analysis, Surf. Sci. 126 (1-3) (1983) 245–252.

[84] J. Quinn, Y.S. Li, D. Tian, H. Li, F. Jona, P.M. Marcus, Anomalous multilayer relaxation of Pd{001}, Phys. Rev. B 42 (17) (1990) 11348–11351.

[85] W. Oed, H. Lindner, U. Starke, K. Heinz, K. Müller, Adsorbate-induced relaxation and reconstruction of c(2× 2) O/Ni (100): A reinvestigation by leed structure analysis, Surf. Sci., 224 (1-3), 989, 179–194.

[86] W. Oed, B. Dötsch, L. Hammer, K. Heinz, K. Müller, A LEED investigation of clean and oxygen covered Rh (100), Surf. Sci., 207 (1), 0000, 55–65.

[87] C.C. Boungou, M. N'dollo, G.B. Bouka-Pivoteau, P.S. Moussounda, T. Dintzer, Density functional studies of the adsorption of OCN and coadsorption of O and CN on Ag(001) surface, Comput. Condens. Matter 22 (2020) e00446–e00454.

[88] J.L.F. Da Silva, C. Stampfl, M. Scheffler, Converged properties of clean metal surfaces by all-electron firstprinciples calculations, Surf. Sci. 600 (3) (2006) 703–715.

[89] P.G. Belelli, G.R. Garda, R.M. Ferullo, DFT study of isocyanate chemisorption on Cu(100): Correlation between substrate–adsorbate charge transfer and intermolecular interactions, Surf. Sci. 605 (13–14) (2011) 1202–1208.

[90] P.G. Belelli, M.M. Branda, G.R. Garda, R.M. Ferullo, N.J. Castellani, Chemisorption of isocyanate (NCO) on the Pd(100) surface at different coverages, Surf. Sci. 604 (3–4) (2010) 442–450.

[91] D.C. Sorescu, Adsorption and activation of CO coadsorbed with K on Fe (100) surface: A plane-wave DFT study, Surf. Sci. 605 (3-4) (2011) 401–414.

[92] M. Kiskinova, G. Pirug, H.P. Bonzel, Coadsorption of potassium and CO on Pt(111), Surf. Sci. 133 (2–3) (1983) 321–343.

[93] S.H. Ma, Z.Y. Jiao, T.X. Wang, A theoretical study for the influence of coverage on Li, Na and K adsorption Co(0001), Comput. Theor. Chem. 963 (1) (2011) 125–129.